Iranian Society of Acoustics and Vibration
The 14th ISAV2024 International Conference on Acoustics and Vibration
11-12 Dec 2024 Karaj - Iran
Kharazmi University

Deep Learning Prediction and Experimental Validation of Nonlinear Acoustic-Driven Flame Dynamics Using a CNN-Transformer Hybrid Model

Mohammad Ali Akhtardanesh[a*], Ensieh Alipour[a],
Mohammad Farshchi[b]

[a] *PhD Candidate, Aerospace Engineering Department, Sharif University of Technology.*

[b] *Full Professor, Aerospace Engineering Department, Sharif University of Technology.*

** Corresponding author e-mail: mohammadali.akhtardanesh@ae.sharif.edu*

Abstract

A hybrid deep learning model combining Convolutional Neural Networks (CNNs) with a Transformer Encoder was proposed to investigate the nonlinear dynamics of a laminar, partially premixed counterflow flame under acoustic excitation. Experimental data from a combustion instability laboratory were used to train the model. OH* chemiluminescence was employed to measure flame responses across frequencies from 20 to 350 Hz and pressure amplitudes up to the extinction threshold. The interactions between acoustic waves and flame dynamics were analysed, revealing the influence of amplitude and frequency variations on heat release rates. Despite dataset limitations, the model accurately approximated the flame transfer function, replicated chemiluminescence signals, and predicted flame responses to diverse acoustic excitations. High-speed imaging and image processing techniques validated the repeatability of flame structures, confirming consistent characteristics across testing cycles. The findings highlighted the potential of the hybrid deep-learning approach for predicting flame dynamics in complex acoustic environments, offering insights for mitigating combustion instabilities in engineering applications.

Keywords: Acoustic wave; deep learning; partially premixed flame; convolutional neural network; encoder of transformer; flame nonlinear response; combustion instability.

---

1. Introduction

Large-amplitude pressure variations caused by thermoacoustic oscillations were found to limit the operational range and increase the risk of fatigue-induced mechanical failure in gas turbine combustors [1], [2]. Optimization approaches aimed at identifying optimal combinations of geometrical and operational parameters were shown to mitigate these instabilities by reducing the likelihood of thermoacoustic instability. Traditionally, adjoint-based techniques—mathematical tools derived from governing equations—were widely employed to evaluate the effects of design or operational changes on thermoacoustic eigenvalues and system stability. Recently, data-driven optimization methods were

employed, as they required no prior knowledge of the system's underlying physics. These black-box approaches assessed performance improvements and iteratively adjusted parameters based on empirical data. A key element in understanding thermoacoustic behaviour was identified as the flame transfer function (FTF), which describes the relationship between fluctuations in the flame's heat release rate and the acoustic inlet velocity [3]–[6]. The FTF characterized the dynamic response of the flame to acoustic excitation, dependent on both the amplitude of velocity fluctuations, $|u'/\bar{u}|$, and the excitation frequency, f. Mathematically, the FTF was expressed as equation (1):

$$FTF(f, |u'/\bar{u}|) = \frac{Q'/\bar{Q}}{U'/\bar{U}} \tag{1}$$

where U′ represented fluctuations in acoustic velocity, $\bar{U}$ denoted the mean flow velocity, Q′ indicated variations in the flame's heat release rate, and $\bar{Q}$ referred to the mean heat release rate. The FTF comprised two components: gain and phase. The gain reflected the amplitude ratio between heat release rate fluctuations and acoustic velocity variations, while the phase represented the time delay or phase shift between acoustic disturbances and the resulting heat release oscillations. In practice, fluctuations in heat release were inferred from optical measurements, such as chemiluminescence, I_{CH} or I_{OH} due to their non-intrusive nature using equation (2) [7].

$$Q'/\bar{Q} = I'/\bar{I} \tag{2}$$

Accurate estimation of the Flame Transfer Function (FTF) is essential for controlling thermoacoustic instabilities and understanding flame dynamics [8]. Traditional models often fail to capture nonlinear behaviors, but machine learning (ML) techniques have shown promise. Advanced architectures, including Transformer encoders, LSTM networks, and physics-informed multi-layer perceptron, have demonstrated improved accuracy in predicting nonlinear flame responses to acoustic excitations [9], [10]. Neural networks have also successfully simulated linear and nonlinear turbulent flame responses to broadband forcing [11]. ML models further predict acoustic power levels required for flame extinction using parameters like frequency, equivalence ratio, wall diameter ratio, and Reynolds number [12]. These studies underscore ML's potential to enhance combustion control, improving safety and performance across diverse conditions.

This research experimentally predicted the FTF of a methane-air flame under acoustic perturbations. Using a test rig, OH* chemiluminescence captured heat release rates, and high-speed imaging validated repeatable parameters, such as flame area, thickness, and heat release position. The deep learning model accurately predicted the nonlinear FTF for both simple and complex signals. By experimentally validating responses across varying frequencies and pressures, this approach enhanced flame response modeling and provided valuable insights into combustion dynamics.

2. Experimental Procedure

2.1 Setup and diagnostics

The experimental setup of the counterflow burner in the Advanced Combustion Laboratory, Sharif University of Technology, is shown in Figure 1 [12]–[14]. The test rig consisted of two identical sections (top and bottom) with a 0.125 mm mesh grid for uniform velocity profiles over a 31.5 cm pipe, along with a converging nozzle, honeycomb plenum, flash-back arrestor, and loudspeaker. Nitrogen co-flowed in the lower section to shield the flame from external disturbances. Loudspeakers (Vibe Black Air 12) generated modulated acoustic waves (20–1200 Hz), measured by an SPL meter (B&K 2250, ±1.5 dB). Acoustic waves were produced via signal generator software, amplified, and delivered to the speakers (Hertz HCP 1DK).

Heat release rate was measured via OH* chemiluminescence [15]. A high-speed CMOS camera (1920 fps, 1280×720 resolution) with a 430 ± 10 nm bandpass filter captured CH* chemiluminescence, while a photomultiplier tube (Thorlabs PMM01) measured instantaneous CH* and OH*

intensities. A microphone monitored the phase lag between photomultiplier signals and acoustic pressure signals. Data were sampled at 3.5 kHz and recorded over 2-second intervals, capturing at least 700 harmonic cycles.

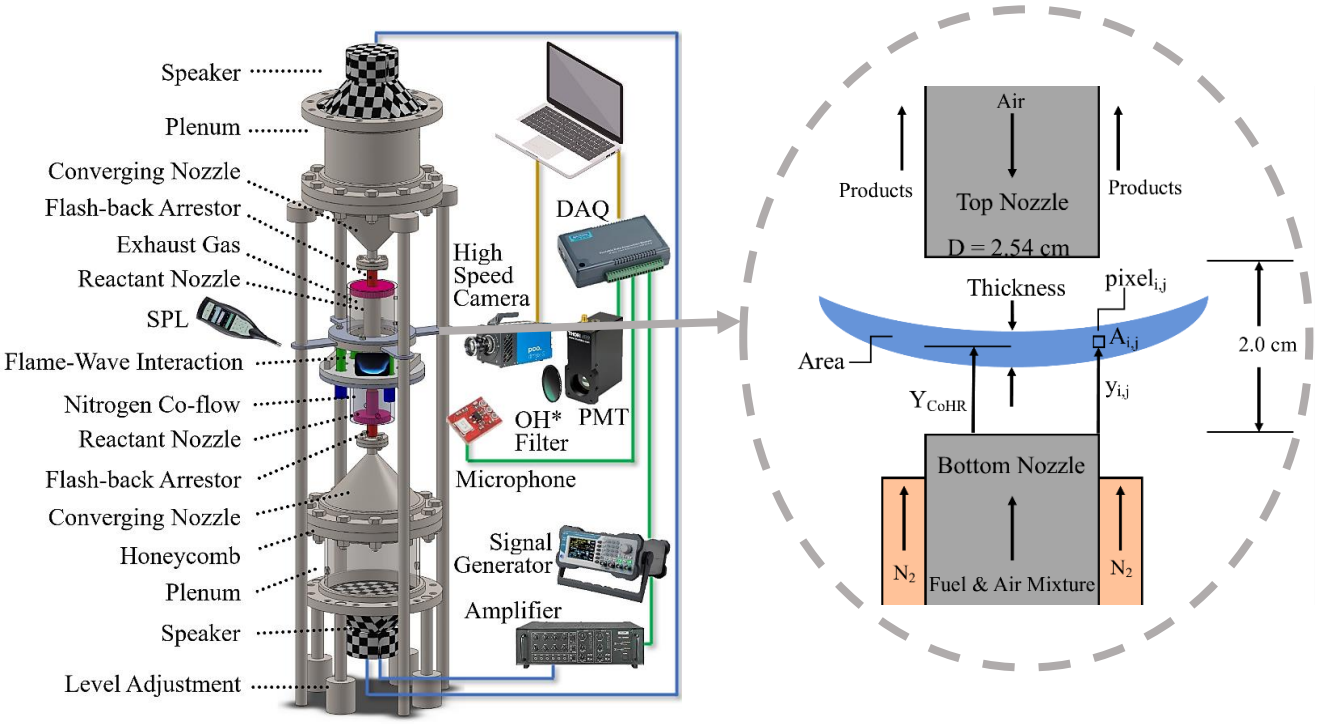

Figure 1. Schematic of the acoustic excitation and diagnostics system integrated into the experimental counterflow flame setup (left) and an illustration depicting the area, thickness, and displacement of the centre of heat release in the counterflow flame (right)

As with any dynamic system, acoustic drivers were characterized by a response function. Experimental tests were conducted to evaluate their ability to generate waves with the desired amplitude and phase. Pressure amplitudes of 3, 5, and 7 Pa were produced across a frequency range of 20–350 Hz by adjusting the acoustic driver's voltage and input current. The phase difference between the signal generator and the acoustic driver was determined using a data acquisition system (DAQ) with a 3500 Hz sampling rate. To prevent interaction between ambient air and nozzle streams, a 99.99% pure nitrogen (N_2) jacket was employed. The nitrogen flow rate was maintained at a minimum of 20 L/min to ensure the flame reaction zone remained undisturbed during acoustic excitations. Air and methane flows were set at 15 L/min and 2.25 L/min, respectively, from the bottom nozzle, while 15 L/min of air was supplied from the top nozzle. This configuration ensured that hydrodynamics and reaction kinetics did not affect the results, isolating flame-acoustic field interactions as the sole variable. The effects of steady harmonic acoustic oscillations with varying amplitudes on partially premixed counterflow flames were analyzed within the frequency range of 20–350 Hz. Higher frequencies were excluded due to flame insensitivity, and lower frequencies were disregarded due to acoustic exciter limitations. With acoustic wavelengths ranging from 17.3 m to 1 m, significantly larger than the flame thickness, the waves interacted with the flame as planar waves inside the burner nozzle.

3. Processing of the experimental data

To analyze the governing physical phenomena, the flame's instantaneous quantities were mathematically defined. As shown in Figure 1, flame thickness was measured as the distance between the highest and lowest pixels of the smoothed image center. Flame surface area was calculated by

counting illuminated pixels (light intensity ≥20 units) and multiplying by their dimensions. Radiation intensity, representing the instantaneous heat release rate, was obtained by integrating pixel brightness at 430 nm, corresponding to CH* emissions. Flame displacement was determined along the central symmetry line using Equation (3), where y_i is the pixel distance from the centre of the lower nozzle, I_i is the pixel radiation intensity at a wavelength of 430 nanometre, and Y_{CoHR} is the centre of the flame radiation area at that moment. The entire process was implemented and executed within an image processing code in MATLAB.

$$Y_{CoHR} = (\sum y_i I_i)/(\sum I_i) \tag{3}$$

To validate repeatability, the flame was tested three times at 40 Hz and 5 Pa. Figure 2 shows high-speed images across 4 frames for 4 cycles and the cycle-averaged image. The Abel inverse transformation [16] derived cross-sectional views, while quantitative results covered CH* intensity fluctuations ($Q'/\bar{Q} \approx I'_{CH}/\bar{I}_{CH}$), flame area, thickness, and heat release center displacement. Errors were below 0.4% for the mean flame surface position and CH* intensity, and below 1.6% for amplitude fluctuations over 100 cycles.

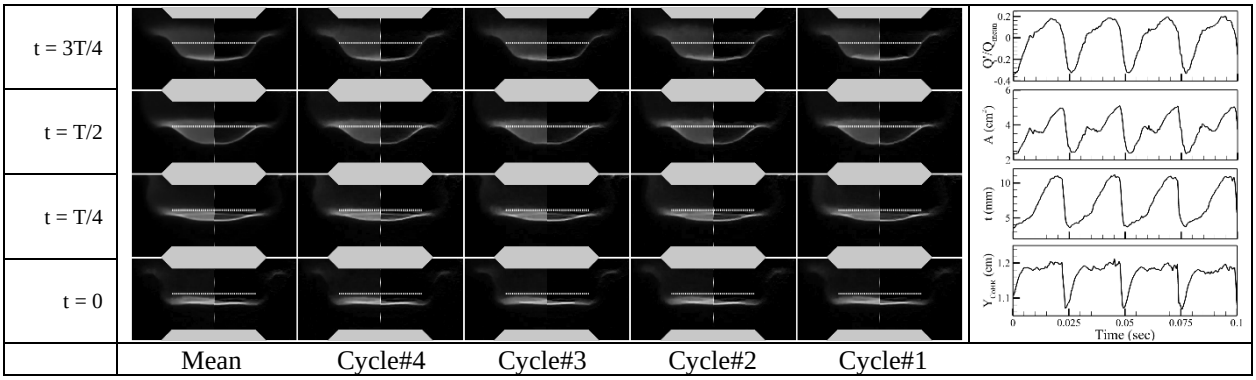

Figure 2. CH* chemiluminescence images and Abel transformations (left) during acoustic excitation (f=40 Hz, P′=5 Pa) over four cycles and as a cycle average. The dashed line marks the stagnation plane. High-speed imaging post process results (right) shows Instantaneous Y_{CoHR}, thickness, area, and the heat release ratio.

Previous studies on premixed flames have demonstrated a direct relationship between flame surface area and heat release rate $Q \propto A$, with linear velocity fluctuations $U'/\bar{U} \ll 1$ showing $Q'/\bar{Q} \sim A'/\bar{A}$ [17]. Chemiluminescence measurements further confirmed a linear correlation between radiation intensity and flame surface area ($\bar{I}_{CH} \propto \bar{A}$), aligning with the observations in Figure 2 and validating the experimental findings. The repeatability of flame-acoustic interactions supports the development of a deep learning model to predict flame responses to acoustic excitation. Training the model across varied acoustic pressures and frequencies would enable the capture of complex nonlinear interactions, enhancing real-time control and prediction of combustion dynamics for more reliable and efficient systems.

4. Deep Learning Model

Traditional signal processing methods fail to capture the complexity of flame dynamics. To address this, a hybrid deep learning model combining Transformer encoders [18] for sequence modeling and CNNs [19] for feature extraction was employed to analyze the flame transfer function and predict system responses to acoustic challenges. The framework (Figure 3) consists of two components: a CNN block with four layers for extracting features from chemiluminescence data and a Transformer Encoder for advanced pattern analysis and forecasting. Early CNN layers capture basic intensity changes, while deeper layers identify complex flame responses to acoustic inputs. Positional

encoding in the Transformer block preserves the temporal sequence of features, enabling the model to capture the flame's sequential response. The self-attention mechanism prioritizes critical input elements for accurate predictions. The attention-weighted features are then processed through a feed-forward network to generate predictions.

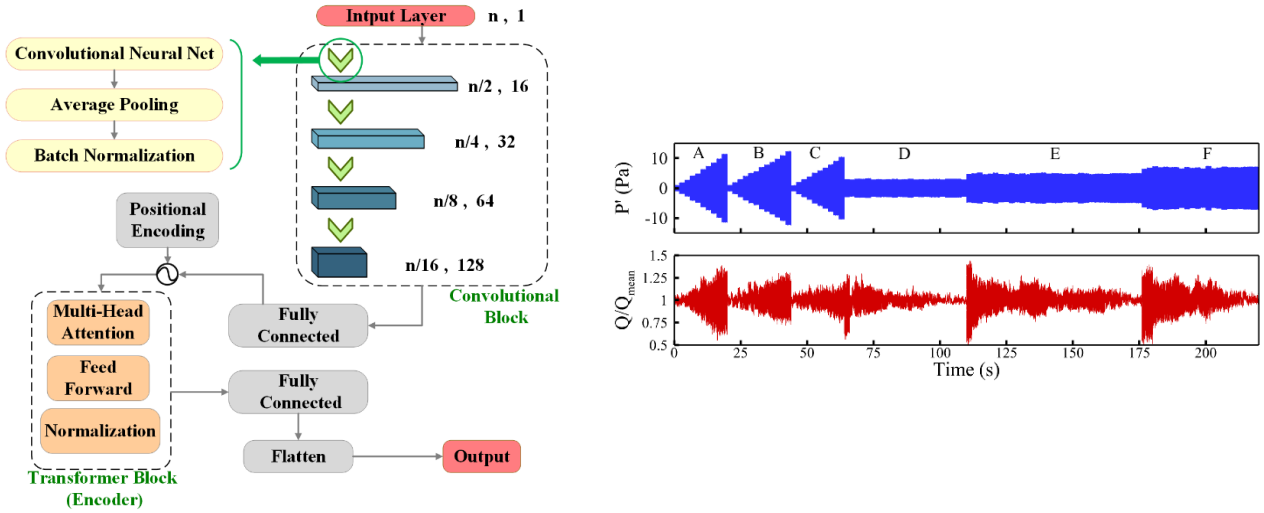

Figure 3. Proposed deep learning model framework for FTF prediction (left) and training data from experiments (right): input acoustic pressure (blue) and corresponding heat release response (red).

4.1 Data Acquisition

Acoustic oscillation frequency and amplitude significantly influence the Flame Transfer Function (FTF). Previous studies noted diminishing oscillation amplitudes near 100 Hz for ethylene flames [20] and structural insensitivity above 200 Hz for methane-air flames [21]. Accordingly, training data were selected from six frequency and amplitude ranges, as shown in Figure 3. The input pressure signal (blue line) and heat release reaction via OH* chemiluminescence (red line) were recorded. For constant-frequency tests (regions A, B, C), amplitudes increased by 1 Pa every two seconds until acoustic extinction, which restricted higher amplitudes [22]–[26]. Region A was conducted at 30 Hz, region B at 60 Hz, and region C at 90 Hz. In variable-frequency tests (regions D, E, F), the frequency spanned 20–350 Hz with amplitudes fixed at 3 Pa, 5 Pa, and 7 Pa, respectively. Each test lasted two seconds, with data sampled at 3500 Hz for both input and output signals.

5. Results and discussion

The model was evaluated using test data with acoustic excitations excluded from training, accurately predicting chemiluminescence signals and closely matching experimental results (Figure 4). For a 30 Hz sinusoidal input at 5 Pa (Figure 4, top), the model captured the mean value, amplitude, and phase with high precision, despite minor deviations due to experimental uncertainties and nonlinear flame-acoustic interactions. Triangular waveforms (Figure 4, middle) produced smoothed outputs, influenced by non-ideal exciter behavior and sensor dynamics. The model demonstrated satisfactory predictive accuracy despite these limitations. Square waveforms (Figure 4, bottom) resulted in distorted outputs due to nonlinear flame dynamics and sensor-actuator constraints. The model accurately predicted phase delay and mean heat release rate, with some variations in amplitude at signal extremums, closely aligning with experimental data.

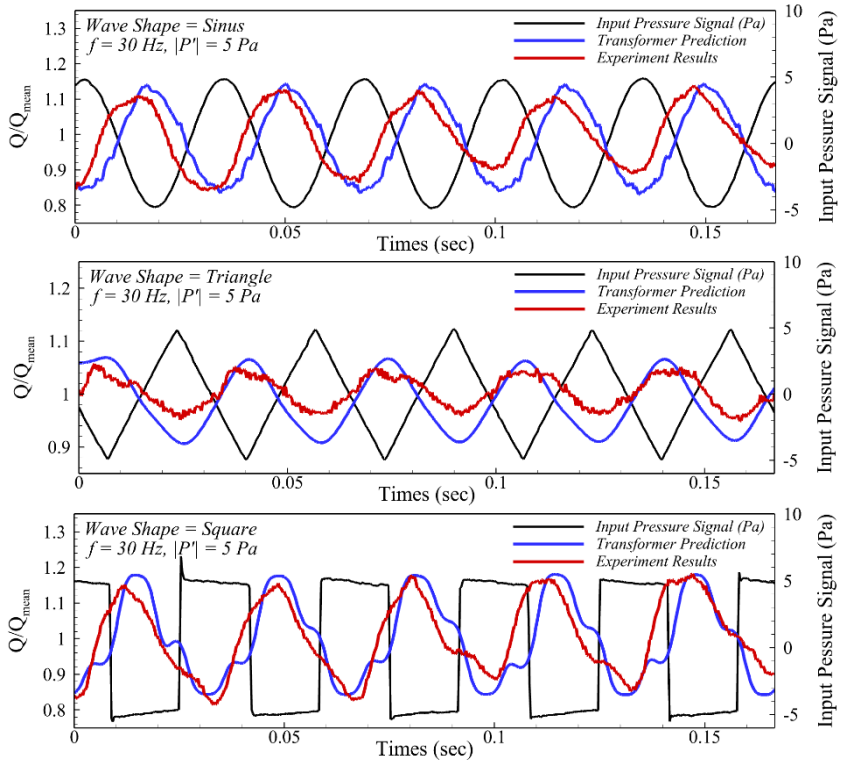

Figure 4. Validation of the square (bottom), the triangle (middle) and the sinus (top) signals at a constant f = 30 Hz and the pressure amplitude of 5 Pa. The black thin line: is the pressure input signal, the blue thick line: is the results predicted by CNNs + Transformer, and the red thick line: is the experimental results

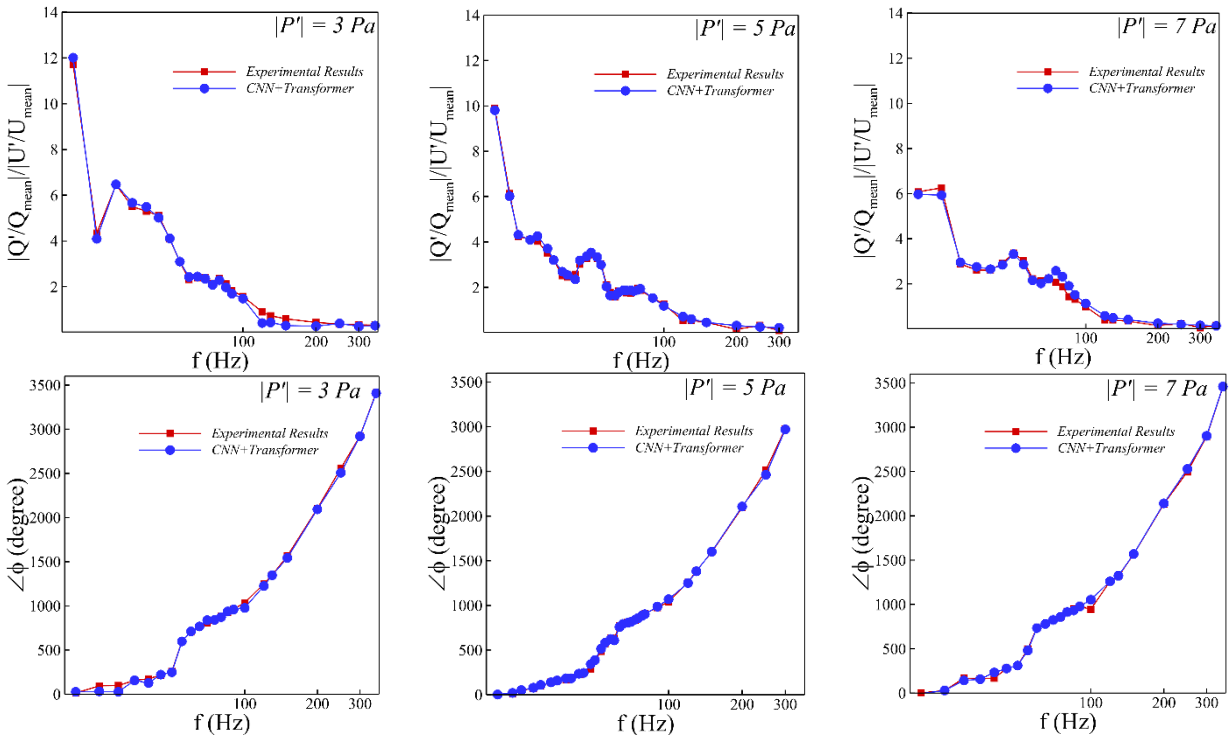

Figure 5. Gain (top) and phase (bottom) of the flame response function for the counterflow flame under varying excitation pressure amplitudes of 3, 5, and 7 Pa. Red squares represent experimental data, while blue circles indicate predictions from the deep learning model.

The analyses so far focused on flame responses under constant pressure or frequency. To assess the model across varying conditions, the flame response function was examined at 3, 5, and 7 Pa over 20–350 Hz. Figure 5 compares the experimentally obtained gain and phase with the deep learning model's predictions. At low frequencies (20 Hz), the flame's heat release oscillations match the order of input acoustic velocity (O(1)), similar to conical flames [27].

The experimental results and the deep learning model exhibited consistent phase and gain across all tested frequencies and pressure amplitudes of the acoustic waves. Within the frequency range of 20 to 150 Hz, the flame response magnitude showed excellent agreement between the two methods, validating the model's ability to capture the flame's dynamic behavior. At frequencies exceeding 150 Hz, both the experimental flame response and the deep learning model prediction converged toward zero. This behavior is notable, as uncertainties in experimental data at higher frequencies, driven by increased sensitivity to environmental disturbances, challenge the model's ability to accurately capture the flame dynamics. To address this limitation, the training dataset for the deep learning model was optimized by reducing the sampling size at higher frequencies. This adjustment effectively minimized the influence of external disturbances, enhancing the model's predictive accuracy in this frequency range. The improved dataset refinement highlights the importance of adapting data preprocessing techniques to achieve robust predictions under varying experimental conditions.

6. Conclusion

This study developed a deep learning framework to predict the dynamic response of a partially premixed methane-air counterflow flame under acoustic excitation. Heat release rates were measured via OH* chemiluminescence across 20–350 Hz and pressure amplitudes up to extinction. A hybrid model combining convolutional neural networks (CNNs) for feature extraction and a Transformer Encoder for sequence forecasting was trained on experimental data, with flame structure repeatability confirmed through high-speed imaging.

The model showed excellent agreement with experimental data, accurately predicting phase and gain across all frequencies and pressure amplitudes. For sinusoidal signals, it closely replicated experimental amplitude, phase, and mean heat release rates, while for triangular and square signals, minor amplitude discrepancies arose due to actuator and sensor limitations. Both experimental and model results exhibited low-pass filter behaviour, with heat release attenuated above 80 Hz and both approaching zero beyond 150 Hz due to experimental uncertainties. Optimizing the training dataset at higher frequencies improved the model's accuracy in capturing high-frequency dynamics.

This framework offers a robust predictive tool for analysing flame response under varying acoustic conditions, providing insights for mitigating combustion instabilities. Future work should focus on enhancing data acquisition rates and refining training datasets to address high-frequency challenges, marking significant progress in applying deep learning to combustion dynamics.

REFERENCES

[1] T. Poinsot, “Prediction and control of combustion instabilities in real engines,” *Proc. Combust. Inst.*, vol. 36, no. 1, pp. 1–28, 2017.

[2] S. Candel, “Combustion dynamics and control: Progress and challenges,” *Proc. Combust. Inst.*, vol. 29, no. 1, pp. 1–28, Jan. 2002.

[3] A. L. Birbaud, D. Durox, S. Ducruix, and S. Candel, “Dynamics of confined premixed flames submitted to upstream acoustic modulations,” *Proc. Combust. Inst.*, vol. 31, no. 1, pp. 1257–1265, Jan. 2007.

[4] T. Schuller, “Self-induced combustion oscillations of laminar premixed flames stabilized on annular burners,” *Combust. Flame*, vol. 135, no. 4, pp. 525–537, Dec. 2003.

[5] D. Durox, T. Schuller, N. Noiray, and S. Candel, “Experimental analysis of nonlinear flame transfer functions for different flame geometries,” *Proc. Combust. Inst.*, vol. 32, no. 1, pp. 1391–1398, 2009.

[6] D. Durox, T. Schuller, and S. Candel, “Combustion dynamics of inverted conical flames,” *Proc.*

Combust. Inst., vol. 30 II, no. 2, pp. 1717–1724, 2005.

[7] M. A. Akhtardanesh, M. Farshchi, M. Ranjbar Najafi, and M. J. Hosseinkhani, "Analysis of CH and OH Chemiluminescense in the Dynamic Study of a Partially Premixed Counterflow Flame," in *Fuel and Combustion (20)*, Tehran: Iranian Society of Fuel and Combustion, 2024.

[8] F. G. Schiavone, A. Aniello, E. Riber, T. Schuller, and D. Laera, "On the adequacy of OH* as heat release marker for hydrogen–air flames," *Proc. Combust. Inst.*, vol. 40, no. 1–4, p. 105248, 2024.

[9] J. Wu, J. Nan, L. Yang, and J. Li, "Reconstruction of the flame nonlinear response using deep learning algorithms," *Phys. Fluids*, vol. 35, no. 1, Jan. 2023.

[10] Y. Shen and A. S. Morgans, "Predicting the effect of hydrogen enrichment on the flame describing function using machine learning," *Int. J. Hydrogen Energy*, vol. 79, no. July, pp. 267–276, 2024.

[11] C. E. Üstün, M. R. Herfatmanesh, A. Valera-Medina, and A. Paykani, "Applying machine learning techniques to predict laminar burning velocity for ammonia/hydrogen/air mixtures," *Energy AI*, vol. 13, no. March, p. 100270, 2023.

[12] M. A. Akhtardanesh, M. J. Hosseinkhani, and M. Farshchi, "The Effect of Hydrogen Addition on the Acoustic Response of a Partially Premixed Counterflow Flame," *Fuel Combust.*, vol. 16, no. 4, pp. 43–60, 2024.

[13] M. A. Akhtardanesh, M. Khadem Alrezaeian, and M. Farshchi, "A Comparison between Methane and Propane Counterflow flame Acoustic Excitation in the Partially Premixed Regime," in *20th Fluid Dynamics Conference*, Tehran: the physics society of iran, 2023.

[14] M. A. Akhtardanesh, M. Khadem Alrezaeian, and M. Farshchi, "Interaction of acoustic waves with a laminar counterflow flame," in *9th National Conference of Acoustical Society of Iran*, Tehran: Acoustical Society of Iran, 2023.

[15] Y. Hardalupas and M. Orain, "Local measurements of the time-dependent heat release rate and equivalence ratio using chemiluminescent emission from a flame," *Combust. Flame*, vol. 139, no. 3, pp. 188–207, 2004.

[16] Y. T. Cho and S. J. Na, "Application of Abel inversion in real-time calculations for circularly and elliptically symmetric radiation sources," *Meas. Sci. Technol.*, vol. 16, no. 3, pp. 878–884, 2005.

[17] S. Schlimpert, M. Meinke, and W. Schröder, "Nonlinear analysis of an acoustically excited laminar premixed flame," *Combust. Flame*, vol. 163, pp. 337–357, 2016.

[18] Y. LeCun, L. Bottou, Y. Bengio, and P. Haffner, "Gradient-based learning applied to document recognition," *Proc. IEEE*, vol. 86, no. 11, pp. 2278–2323, 1998.

[19] A. Vaswani, "Attention Is All You Need," no. Nips, 2017.

[20] T. SAITOH and Y. OTSUKA, "Unsteady Behavior of Diffusion Flames and Premixed Flames for Counter Flow Geometry," *Combust. Sci. Technol.*, vol. 12, no. 4–6, pp. 135–146, Apr. 1976.

[21] T. M. Brown and R. W. Pitz, "Experimental investigation of counterflow diffusion flames with oscillatory stretch," in *34th Aerospace Sciences Meeting and Exhibit*, Reston, Virigina: American Institute of Aeronautics and Astronautics, Jan. 1996. doi: 10.2514/6.1996-214.

[22] M. A. Akhtardanesh, M. Khadem Alrezaeian, M. J. Hosseinkhani, and M. Farshchi, "An experimental study on Bunsen flame acoustic extinction," in *The 21st International Conference of Iranian Aeropace Association*, Tehran, 2022.

[23] M. A. Akhtardanesh, M. J. Hosseinkhani, and M. Farshchi, "Acoustic Extintion of Partially Premixed Counterflow flame," in *20th Fluid Dynamics Conference*, Tehran: the physics society of iran, 2023.

[24] E. Alipour, M. A. Akhtardanesh, and S. M. B. Malaek, "Application of Machine Learning to Bring Efficiency to Costly Experiments ; Case of Flame-Extinction," in *Fuel and Combustion (20)*, Tehran: Iranian Society of Fuel and Combustion, 2024.

[25] M. A. Akhtardanesh, M. J. Hosseinkhani, and M. Farshchi, "Acoustic Extinction of Partially Premixed Counterflow flame," *J. Engine Res.*, vol. 70, no. 3, pp. 39–52, 2023.

[26] M. A. Akhtardanesh, E. Alipour, and S. M. B. Malaek, "Application of Machine Learning to Bring Efficiency to Costly Experiments: Case of Flame-Extinction," *Fuel Combust.*, vol. 17, no. 2, pp. 20–36, 2024.

[27] W. Polifke and C. Lawn, "On the low-frequency limit of flame transfer functions," *Combust. Flame*, vol. 151, no. 3, pp. 437–451, Nov. 2007.